Journal of Physiology (1989), **416**, *pp.* 141–160
With 13 *text-figures*
Printed in Great Britain

LOW-VOLTAGE-ACTIVATED CALCIUM CURRENT IN RAT AORTA SMOOTH MUSCLE CELLS IN PRIMARY CULTURE

BY NORIO AKAIKE*, HIDEO KANAIDE†, TAKESHI KUGA, MOTOOMI NAKAMURA‡, JUN-ICHI SADOSHIMA AND HITONOBU TOMOIKE

*From the Research Institute of Angiocardiology and Cardiovascular Clinic, †Division of Molecular Cardiology and the *Department of Physiology, Faculty of Medicine, Kyushu University 71, Fukuoka 812, Japan*

(*Received 16 December 1988*)

SUMMARY

1. Electrical and pharmacological properties of the low-voltage-activated Ca^{2+} current ($I_{Ca,\,LVA}$) in rat aorta smooth muscle cells (SMC) in primary culture were examined, particularly in comparison with the high-voltage-activated Ca^{2+} current ($I_{Ca,\,HVA}$). Both types of Ca^{2+} currents were recorded in external solution containing 20 mM-Ca^{2+}, using the whole-cell voltage-clamp technique.

2. $I_{Ca,\,LVA}$ was evoked by step depolarizations to potentials more positive than −60 mV from a holding potential of −100 mV, and reached a peak in the current–voltage (*I–V*) relationship around −30 mV. $I_{Ca,\,HVA}$ was activated at −20 mV, and reached a peak at +20 mV.

3. The intracellular dialysis of 5 mM-F^- irreversibly suppressed $I_{Ca,\,HVA}$, with time, while it has little effect on the $I_{Ca,\,LVA}$. The $I_{Ca,\,LVA}$ could be separated from the $I_{Ca,\,HVA}$ by either selecting the holding and test potential levels or by perfusing intracellularly with F^-.

4. The ratio of peak amplitude of Ba^{2+}, Sr^{2+} and Ca^{2+} currents in the respective *I–V* relationship was 1·6:1·2:1·0 for high-voltage-activated Ca^{2+} channels and was 1·0:1·4:1·0 for low-voltage-activated ones.

5. The inactivation phase of $I_{Ca,\,HVA}$ was fitted by a sum of double-exponential functions, the time constants of which were larger when the current was carried by Ba^{2+} than by Ca^{2+}. The inactivation time course of $I_{Ca,\,LVA}$ was fitted by a single-exponential function, and the time constant was practically the same when the current was carried by Ba^{2+} or by Ca^{2+}. Activation and inactivation processes of $I_{Ca,\,LVA}$ were potential-dependent.

6. The steady-state inactivation curve of $I_{Ca,\,LVA}$ was fitted by the Boltzmann equation, having a mid-potential of −80 mV and a slope factor of 5·0. The recovery time course from steady-state inactivation was fitted by a sum of two exponential functions. The time constants of the faster phase were 230 and 380 ms, and those of slower phase were 2·8 and 1·8 s at the repolarization potentials of −120 and −100 mV, respectively.

‡ To whom reprint requests should be addressed.

7. The amplitude of $I_{Ca,\,LVA}$ depended on the external Ca^{2+} concentration ($[Ca^{2+}]_o$), approaching saturation at 95 mM $[Ca^{2+}]_o$.

8. Various polyvalent cations blocked both types of Ca^{2+} current reversibly in the order (IC_{50} in M): La^{3+} (8×10^{-8}) > Cd^{2+} (6×10^{-6}) > Ni^{2+} (1×10^{-5}) > Zn^{2+} (3×10^{-5}) for $I_{Ca,\,HVA}$, and La^{3+} (6×10^{-7}) > Zn^{2+} (3×10^{-5}) > Cd^{2+} (4×10^{-4}) > Ni^{2+} (6×10^{-4}) for $I_{Ca,\,LVA}$.

9. Both types of Ca^{2+} currents were also sensitive to organic Ca^{2+} antagonists, in the following sequence (IC_{50} in M): flunarizine (1×10^{-7}) > nicardipine (2×10^{-7}) > verapamil (9×10^{-7}) > diltiazem (3×10^{-6}) for $I_{Ca,\,HVA}$, and flunarizine (2×10^{-7}) > nicardipine (8×10^{-7}) > nifedipine (3×10^{-6}) > diltiazem (3×10^{-5}) > verapamil (7×10^{-5}) for $I_{Ca,\,LVA}$. Bay K 8644 (10^{-6} M) produced about 3-fold augmentation of $I_{Ca,\,HVA}$ while it had no effects on $I_{Ca,\,LVA}$.

10. With prolongation of the period of cell culture, the population of cells having $I_{Ca,\,LVA}$ decreased and those having $I_{Ca,\,HVA}$ increased.

11. It was concluded that rat aorta SMC in primary culture possessed a definite class of low-voltage-activated Ca^{2+} channels, which was characterized by a high sensitivity to some Ca^{2+} antagonists such as flunarizine and nicardipine.

INTRODUCTION

The presence of low-voltage-activated (T-type) Ca^{2+} channels has been noted in different cells, including vascular smooth muscle cells (SMC) (rat mesenteric artery: Bean, Sturek, Puga & Hermsmeyer, 1986; rat aortic A10 cell line: Friedman, Kurtz, Kaczorowski, Kats & Reuben, 1986; rat aortic A7r5 cell line: Fish, Sperti, Colucci & Clapham, 1988; rat azygos vein: Sturek & Hermsmeyer, 1986; rabbit ear artery: Benham, Hess & Tsien, 1987; rat portal vein: Loirand, Pacaud, Mironneau & Mironneau, 1986; canine saphenous vein: Yatani, Seidel, Allen & Brown, 1987). Since the low-voltage-activated Ca^{2+} channel is activated around the resting potential level of vascular SMC, it might play an important role in the control of intracellular Ca^{2+}-dependent processes such as regulation of vascular tone. However, a systematic study of the low-voltage-activated Ca^{2+} current ($I_{Ca,\,LVA}$) has apparently not been done on vascular SMC, perhaps because, in vascular SMC, the $I_{Ca,\,LVA}$ has a small amplitude and is usually contaminated by the 'classical' high-voltage-activated (L-type) Ca^{2+} current ($I_{Ca,\,HVA}$) around the peak membrane potential.

In the present study, we used rat aorta SMC in primary culture in an attempt to characterize $I_{Ca,\,LVA}$ by the whole-cell voltage-clamp method. Since $I_{Ca,\,LVA}$ in this preparation was significantly larger than $I_{Ca,\,HVA}$, this preparation had an advantage for characterization of $I_{Ca,\,LVA}$. In addition, an intracellular application of a low concentration of F^- enabled isolation of $I_{Ca,\,LVA}$, with no effect on $I_{Ca,\,LVA}$. Detailed analyses of voltage dependence, current kinetics, ionic selectivities and pharmacological properties of $I_{Ca,\,LVA}$ were made in comparison with those of $I_{Ca,\,HVA}$ in vascular SMC. Developmental changes of $I_{Ca,\,LVA}$ in cultured SMC were also investigated.

METHODS

Preparations. Wistar rats (200–250 g) were anaesthetized and killed by ether and SMC of aortic media were dispersed enzymatically and grown in primary culture, as described by Yamamoto, Kanaide & Nakamura (1983). The direct immunofluorescence staining of smooth muscle myosin and actin excluded the contamination of fibroblasts (Kobayashi, Kanaide & Nakamura, 1985).

Electrical measurements. On days 5–15, vascular SMC cultured on a cover-slip were trypsinized for 1 min to clean the surface and to remove interactions among the cells. The cultured cells on the cover-slip were then placed in a recording chamber and continuously superfused with external solution at the rate of 1 ml/min. The whole-cell voltage-clamp method (Hamill, Marty, Neher, Sakmann & Sigworth, 1981) was used. The tip resistance of a heat-polished patch pipette was 2–5 MΩ when it was filled with internal solution. After obtaining a giga-seal between the pipette tip and

TABLE 1. Composition of solution (mM)

External solution

	$CaCl_2$	$BaCl_2$	$SrCl_2$	Tris-Cl	NaCl	KCl	HEPES	TEA-Cl	4-AP	Glucose
5 Ca^{2+}	5	—	—	—	132	2	5	15	2	10
10 Ca^{2+}	10	—	—	—	125	2	5	15	2	10
20 Ca^{2+}	20	—	—	—	110	2	5	15	2	10
50 Ca^{2+}	50	—	—	—	65	2	5	15	2	10
95 Ca^{2+}	95	—	—	—	—	2	5	15	2	10
20 Ba^{2+}	—	20	—	—	110	2	5	15	2	10
20 Sr^{2+}	—	—	20	—	110	2	5	15	2	10
Tris	—	—	—	20	110	2	5	15	2	10

The pH was adjusted to 7·3 with Tris base.

Internal solution

	NMG	HF	Na_2ATP	$MgSO_4$	TEA-Cl	HEPES	Tris-OH	GEDTA	Cyclic AMP
5 F^-	110	5	5	5	20	5	2	10	1
F^--free	110	—	5	5	20	5	2	10	1

The pH was adjusted to 7·2 with HCl.

the cell membrane, the patch membrane was ruptured by pulses of gentle suction. The currents were amplifed with a patch-clamp amplifier (List-Electronic, EPC-7, FRG) with capacitance and series-resistance compensation, filtered at 2·0 kHz, digitized at 5 kHz and analysed with a computer (NEC, PC-9801XL, Japan). All experiments were monitored on a digital storage oscilloscope (Iwatsu, DS-6121A, Japan) and were simultaneously stored on a PCM data recorder (NF Circuit Design Block, RP-880, Japan) for further analyses.

The amplitude of inward current was measured at the peak of each current, in which the leakage current was corrected. The leakage current evoked by a hyperpolarization was subtracted from the current evoked by a depolarization of equal size.

Solutions. The ionic compositions of the solutions used are listed in Table 1. We used extracellular solution containing 20 mM-Ca^{2+}, unless otherwise stated. The concentration of Ca^{2+}, in the external solution was increased by isosmotic substitution of $CaCl_2$ for NaCl. When examining $I_{Ca,LVA}$, we used internal solution containing 5 mM-F^-. To record $I_{Ca,HVA}$, however, we perfused the cells with an internal solution containing no F^-. The volume of the chamber was 0·7 ml. The external solution was changed by gravity at the rate of 7 ml/min. Exchange of the external solution was accomplished within 60 s. All experiments were carried out at room temperature (~ 22–24 °C).

Drugs. The drugs used were trypsin (GIBCO, USA), flunarizine (Kyowa Hakko, Japan), nicardipine (Yamanouchi, Japan), Bay K 8644, nifedipine (Bayer, FRG), diltiazem (Tanabe,

Japan), verapamil (Eisai, Japan), ω-conotoxin GVIA (Peptide Institute, Japan), amiloride (Sigma, USA) and *N*-methyl-D-glucamine (NMG; Tokyo Kasei, Japan).

Some drugs were prepared as a stock solution and were made to a final concentration with an external solution containing 20 mM-Ca^{2+}. Dihydropyridine derivatives were dissolved in 99% ethanol to make a 1 mM stock solution and were protected from exposure to light. At the concentration used, ethanol had no effects on either $I_{Ca,\,LVA}$ or $I_{Ca,\,HVA}$.

Statistics. Data are given as mean ±S.E.M. (n = number of experiments.) Theoretical curves were fitted to the experimental data using the least-squares method. Tests of significance were performed using Student's t test.

RESULTS

Two types of Ca^{2+} currents

Figure 1 shows the inward currents of the rat aorta SMC in primary culture, as recorded in a 20 mM-Ca^{2+} external solution. To suppress the outward K^+ currents, we used an external solution containing tetraethylammonium chloride (TEA) and 4-aminopyridine (4-AP) and an internal solution containing *N*-methyl-D-glucamine (NMG) and TEA. Neither 60 μM-tetrodotoxin nor a substitution of extracellular Na^+ by $Tris^+$ decreased these inward currents. The inward currents were abolished by 1 mM-La^{3+} and increased by increasing the extracellular Ca^{2+} concentration (see Fig. 9), thereby indicating that the currents were carried through Ca^{2+} channels (Akaike, Lee & Brown, 1978).

There are three kinds of cell types classified according to the difference in the inward currents. Figure 1 shows how we identified the cell type. In the first type, a depolarization to −30 mV from a holding potential (V_H) of −100 mV (step *a*) elicited a transient Ca^{2+} current but a depolarization to +20 mV from a V_H of −60 mV (step *b*) elicited no inward current (Fig. 1*A*). Since the transient Ca^{2+} current was elicited at relatively low membrane potential and kinetic characteristics are identical to the low-voltage-activated Ca^{2+} current first reported by Carbone & Lux (1984), this transient Ca^{2+} current was termed low-voltage-activated Ca^{2+} current ($I_{Ca,\,LVA}$). We identified that this type of cell had only low-voltage-activated Ca^{2+} channels. In the second type of cell, step *a* elicited no inward current but step *b* elicited a slowly inactivating inward current (Fig. 1*B*). Since this slowly inactivating Ca^{2+} current was activated at a higher membrane potential than $I_{Ca,\,LVA}$, this current was termed high-voltage-activated Ca^{2+} current ($I_{Ca,\,HVA}$). We identified that this type of cell had only high-voltage-activated Ca^{2+} channels. In the third cell type, step *a* elicited a transient inward current identical to $I_{Ca,\,LVA}$ and step *b* elicited a slowly inward current identical to $I_{Ca,\,HVA}$ (Fig. 1*C*). We identified that this type of cell had both low- and high-voltage-activated Ca^{2+} channels.

Figure 2*A* shows a typical $I_{Ca,\,LVA}$ recorded from the cell having only low-voltage-activated Ca^{2+} channels. $I_{Ca,\,LVA}$ appeared around −60 mV and reached a peak value at about −30 mV in the current–voltage (I–V) relationship. The peak value was 140 ± 19 pA (n = 40). Figure 2*B* shows a typical $I_{Ca,\,HVA}$ recorded from the cell having only high-voltage-activated Ca^{2+} channels. The $I_{Ca,\,HVA}$ was activated at about −20 mV and reached a peak at about +20 mV. The peak value of $I_{Ca,\,HVA}$ was 93 ± 10 pA (n = 40). The peak amplitude of $I_{Ca,\,LVA}$ was significantly larger than that of $I_{Ca,\,HVA}$ ($P < 0.05$).

Separation of two types of Ca^{2+} current

We could select cells having only $I_{Ca,\,LVA}$ to characterize $I_{Ca,\,LVA}$, as shown in Fig. 1. However, when we needed exclusively to avoid contamination of $I_{Ca,\,HVA}$ in analyses of the activation and inactivation kinetics or pharmacological examinations, we used an internal solution containing F^-. An intracellular dialysis with F^- irreversibly suppressed $I_{Ca,\,HVA}$ in neurones (Akaike, Nishi & Oyama, 1983; Carbone

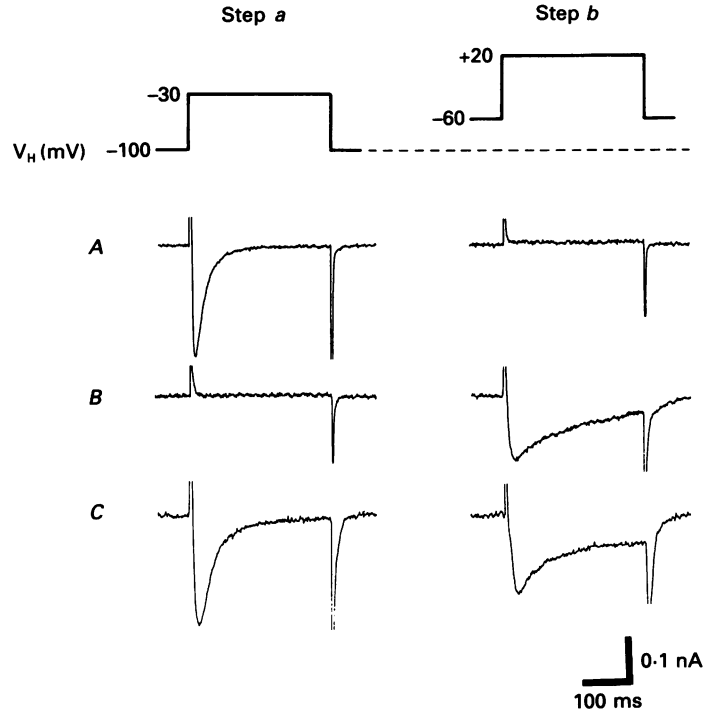

Fig. 1. Identification of the type of Ca^{2+} current. Upper trace shows two kinds of step depolarizations applied to a single cell. Values of the membrane potentials are described at the left of each trace. *A*, recordings taken from a cell showing only low-voltage-activated Ca^{2+} current ($I_{Ca,\,LVA}$). *B*, a cell showing only high-voltage-activated Ca^{2+} current ($I_{Ca,\,HVA}$). *C*, a cell showing both $I_{Ca,\,LVA}$ and $I_{Ca,\,HVA}$. $[Ca^{2+}]_o$, 20 mM.

& Lux, 1987). To make the direct effect of F^- on $I_{Ca,\,LVA}$ minimal, we used a low concentration of F^-. Figure 3 shows the relationship between the duration of perfusion of internal solutions, with and without 5 mM-F^-, and the relative amplitude of I_{Ca}. The $I_{Ca,\,HVA}$ was completely suppressed by the internal perfusion of F^- for 15 min, while neither the amplitude nor kinetics of $I_{Ca,\,LVA}$ was affected by the F^- perfusion, for at least 30 min. The presence of intracellular F^- shifted the *I–V* relationship to negative membrane potentials by only 5 mV (not shown). Thus, we used an internal solution containing 5 mM-F^- when examining $I_{Ca,\,LVA}$. To investigate $I_{Ca,\,HVA}$ we used an internal solution with no F^- and set the V_H at -60 mV. In addition, we could minimize the 'run-down' of $I_{Ca,\,HVA}$ by an internal dialysis of 5 mM-ATP, 1 mM-cyclic AMP, 5 mM-Mg^{2+} and 10 mM-glycolether diamine-tetraacetic acid (GEDTA) for at least 30 min (Irisawa & Kokubun, 1983).

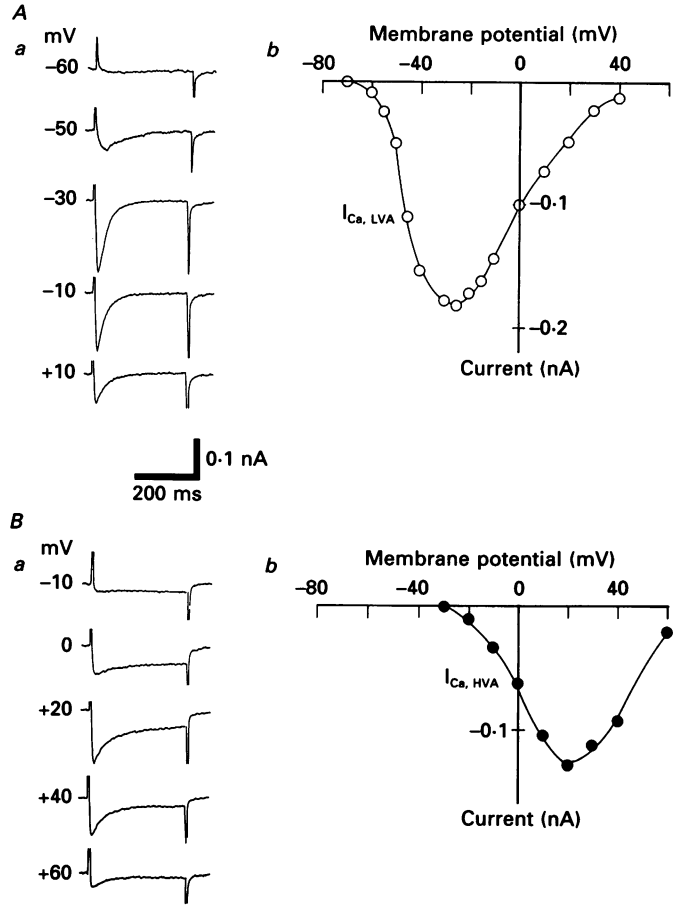

Fig. 2. Two types of Ca^{2+} currents in rat aorta smooth muscle cells in primary culture. *Aa*, an example of $I_{Ca, LVA}$ recordings at the test potentials indicated nearby. *Ab*, the current–voltage (*I–V*) relationship of the same cell. The data are representative of forty experiments. *Ba*, an example of $I_{Ca, HVA}$. *Bb*, *I–V* relationship of the same cell. The leakage currents were subtracted. The holding potential (V_H) was −100 mV. The external Ca^{2+} concentration ($[Ca^{2+}]_o$) was 20 mM. The data are representative of forty experiments.

Ionic selectivities

Ionic selectivities of both types of Ca^{2+} channels were estimated from the peak inward currents in external solutions containing 20 mM-Ba^{2+} or Sr^{2+}, in an equimolar substitution for Ca^{2+}. The amplitude of $I_{Ca, HVA}$ was considerably increased by replacement of extracellular Ca^{2+} with Sr^{2+} or Ba^{2+} (Fig. 4*Aa*). On the other hand, the replacement of extracellular Ca^{2+} with Sr^{2+} induced a significant increase in the amplitude of $I_{Ca, LVA}$, but that with Ba^{2+} little affected the amplitude (Fig. 4*Ba*). Figure 4*Ab* and *Bb* shows the current–voltage (*I–V*) relationships of Ca^{2+}, Ba^{2+} or Sr^{2+} currents carried through two types of Ca^{2+} channels. The ratios of I_{Ba}, I_{Sr} and I_{Ca} at the peak values were 1·6:1·2:1·0 for the high-voltage-activated Ca^{2+} channels

($n = 4$) and 1·0 : 1·4 : 1·0 for the low-voltage-activated ones ($n = 4$). In both types of currents, the membrane potentials of the peak current of I_{Ba} and I_{Sr} in the respective I–V relationships were 10 mV more negative than that of I_{Ca}.

Analysis of inactivation

Figure 5 shows semilogarithmic plots of the inactivation phase of high- and low-voltage-activated currents. Inactivation of the high-voltage-activated current was fitted by a sum of double-exponential functions. We named the time constant for the

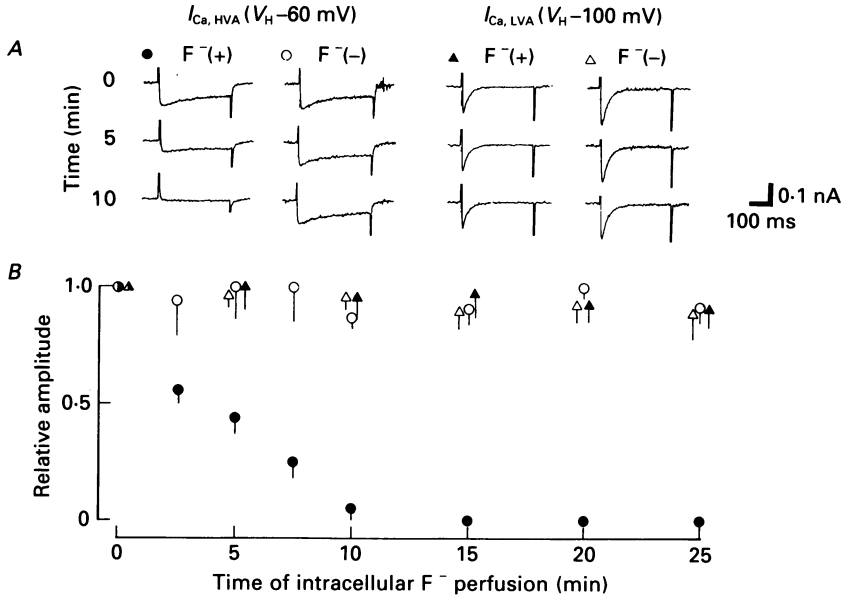

Fig. 3. Effect of internal perfusion of 5 mM-F^- on $I_{Ca, HVA}$ and $I_{Ca, LVA}$. *A*, recordings of $I_{Ca, HVA}$ and $I_{Ca, LVA}$, with (+) or without (−) internal F^-. The records were obtained from four different cells. The time after the first application of the test pulse is indicated. $[Ca^{2+}]_o$, 20 mM. *B*, the time course of the amplitude of $I_{Ca, HVA}$ with (●) and without (○) internal F^-, and $I_{Ca, LVA}$ with (▲) and without (△) F^-. All currents were normalized for the individual peak amplitudes at time zero. Data are mean ±S.E.M. Each point is the average from five cells.

faster falling phase τ_{h1} (Fig. 5*Ab*) and that for the slower falling phase τ_{h2} (Fig. 5*Aa*). As shown in Fig. 5*A*, both time constants of $I_{Ba, HVA}$ were larger than those of $I_{Ca, HVA}$. Inactivation of the low-voltage-activated current was fitted by a single-exponential function, regardless of whether the current was carried by Ca^{2+} or by Ba^{2+}, and the inactivation of $I_{Ca, LVA}$ and $I_{Ba, LVA}$ had an almost equal time constant (Fig. 5*B*).

Voltage- and time-dependent characteristics of $I_{Ca, LVA}$

The kinetic properties of $I_{Ca, LVA}$ were analysed by measuring the activation time (time to peak, t_p) and the inactivation time (decay time constant, τ_h) at different test potentials. The time to peak and the decay time constant of $I_{Ca, LVA}$ are plotted

against the membrane potential (Fig. 6). Both activation and inactivation of $I_{Ca,\,LVA}$ were strongly potential-dependent. Both t_p and τ_h decreased with increasing depolarization.

The activation curve of $I_{Ca,\,LVA}$ is shown in Fig. 7*A*. The maximum activation level was assumed to be the value extrapolated from the linear part of the *I–V* curve. $I_{Ca,\,LVA}$ was activated at a threshold membrane potential of −60 mV, and reached full activation at −15 mV.

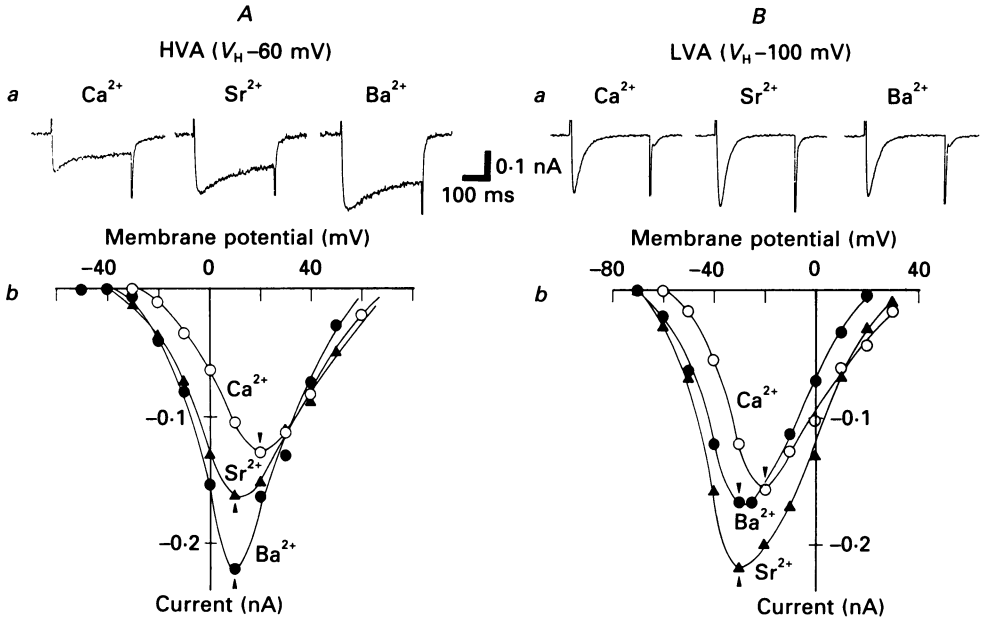

Fig. 4. Ionic selectivities of two types of Ca^{2+} current. *Aa*, maximum HVA currents carried by Ca^{2+}, Sr^{2+} and Ba^{2+}. Test potentials for Ca^{2+}, Sr^{2+} and Ba^{2+} were +20, +10 and +10 mV, respectively, and are shown by the small arrows on the individual *I–V* relationship in *b*. *Ab*, typical *I–V* relationships of HVA currents carried by Ca^{2+}, Sr^{2+} and Ba^{2+}. The V_H was −60 mV. The data are representative of four reproducible experiments. *Ba*, maximum LVA currents carried by Ca^{2+}, Sr^{2+} and Ba^{2+}. Test potentials for Ca^{2+}, Sr^{2+} and Ba^{2+} were −20, −30 and −30 mV, respectively, and are shown by the small arrows on the individual *I–V* relationships in *b*. *Bb*, representative *I–V* relationships of LVA currents carried by Ca^{2+}, Sr^{2+} and Ba^{2+}. The V_H was −100 mV. The data are representative of four reproducible experiments. The current traces in *A* and *B* were obtained from different cells. The concentration of the external divalent cation was 20 mM.

The steady-state inactivation of $I_{Ca,\,LVA}$ was measured using the double-pulse method with a V_H of −120 mV (Fig. 7*B*). The obtained h–V_m curve was fitted by Boltzmann's equation,

$$h(V_m) = 1/\{1+\exp(V_m - V_{0.5})/k\},$$

where V_m is the pre-pulse membrane potential, $V_{0.5}$ is the mid-potential and k is the slope factor of the curve. When the duration of the pre-pulse was 100 ms, $I_{Ca,\,LVA}$ was completely suppressed at a pre-pulse potential of −20 mV. At more positive pre-

pulse potentials, the amplitude of $I_{Ca,\,LVA}$ did not increase, a phenomenon differing from that seen with $I_{Ca,\,HVA}$ with a voltage- and current-dependent inactivation mechanism (Akaike, Nishi & Oyama, 1981*b*; Brown, Morimoto, Tsuda & Wilson, 1981). When the duration of the pre-pulse was prolonged, the curve shifted towards the left. However, $V_{0.5}$ was little changed by prolonging the pre-pulse by more than 3 s ($V_{0.5}$ was −77 mV at 3 s and −80 mV at 10 s).

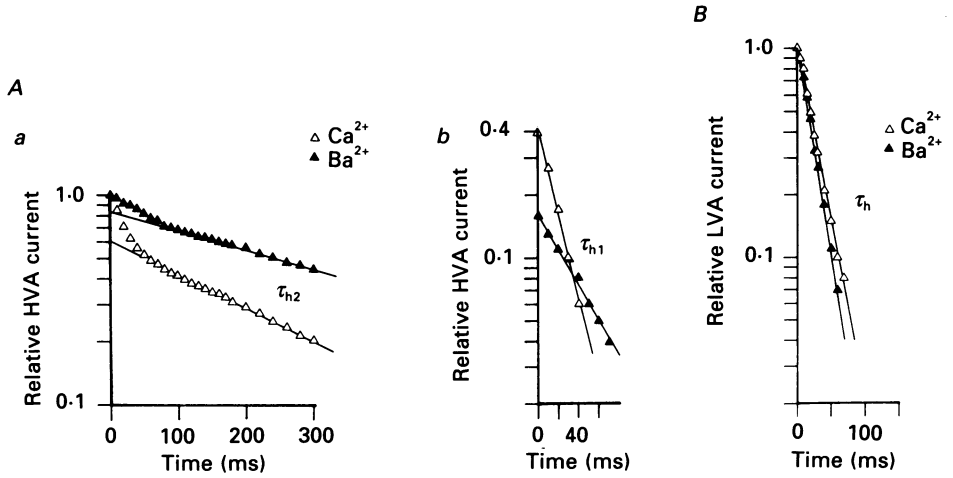

Fig. 5. Inactivation of two types of Ca^{2+} channels in which the currents were carried by Ca^{2+} or Ba^{2+}. Kinetic analysis was made on each peak amplitude of Ca^{2+} and Ba^{2+} currents. Data were quoted from Fig. 4*Aa* and *Ba* and are representative of ten experiments. *Aa*, semilogarithmic plots of the slower components of the inactivation of $I_{Ca,\,HVA}$ (△) and $I_{Ba,\,HVA}$ (▲). In this example, time constants (τ_{h2}) for the slower components of $I_{Ca,\,HVA}$ and $I_{Ba,\,HVA}$ were 275 and 440 ms, respectively. *Ab*, semilogarithmic plots of the faster component of the $I_{Ca,\,HVA}$ (△) and $I_{Ba,\,HVA}$ (▲). In this case, time constants (τ_{h1}) for the faster components of $I_{Ca,\,HVA}$ and $I_{Ba,\,HVA}$ were 21 and 52 ms, respectively. *B*, semilogarithmic plots of $I_{Ca,\,LVA}$ (△) and $I_{Ba,\,LVA}$ (▲). The time constants (τ_h) for $I_{Ca,\,LVA}$ and $I_{Ba,\,LVA}$ were 20 and 18 ms, respectively. The V_H was −60 mV for HVA current and −100 mV for LVA current. The external Ca^{2+} or Ba^{2+} concentration was 20 mM.

Figure 8 shows recovery time courses of $I_{Ca,\,LVA}$ from the inactivation at different repolarization potentials (V_t). The $I_{Ca,\,LVA}$ was completely inactivated by a pre-pulse of 200 ms or 3 s duration, at a membrane potential of −30 mV. When the duration of the pre-pulse was 200 ms, the recovery from inactivation could be fitted by a single-exponential function. The time constants at V_t of −120 and −100 mV were 70 and 140 ms, respectively (Fig. 8*A*). When the duration of the pre-pulse was prolonged to 3 s, the recovery was fitted by a sum of two exponential functions. The time constants at a V_t of −120 mV were 230 ms and 2·8 s, and those at a V_t of −100 mV were 380 ms and 1·8 s (Fig. 8*B*).

Extracellular Ca^{2+} dependence of $I_{Ca,\,LVA}$

The *I–V* relationships of $I_{Ca,\,LVA}$ were plotted as a function of $[Ca^{2+}]_o$ (Fig. 9*A*). An increase in $[Ca^{2+}]_o$ produced an increase in the amplitude of $I_{Ca,\,LVA}$ and shifted the *I–V* relationship in the positive direction, which was about a 25 mV per 10-fold

$[Ca^{2+}]_o$ increase from 5 to 50 mM. When the peak amplitude of $I_{Ca,\,LVA}$ in the respective I–V curves was plotted against $[Ca^{2+}]_o$, a definite trend towards saturation was observed, thereby suggesting the existence of saturable binding sites for Ca^{2+} within low-voltage-activated Ca^{2+} channels (Carbone & Lux, 1987) as well as high-voltage-activated Ca^{2+} channels (Yasui & Akaike, 1986). However, the saturation was not complete even at 95 mM $[Ca^{2+}]_o$ (Fig. 9*B*).

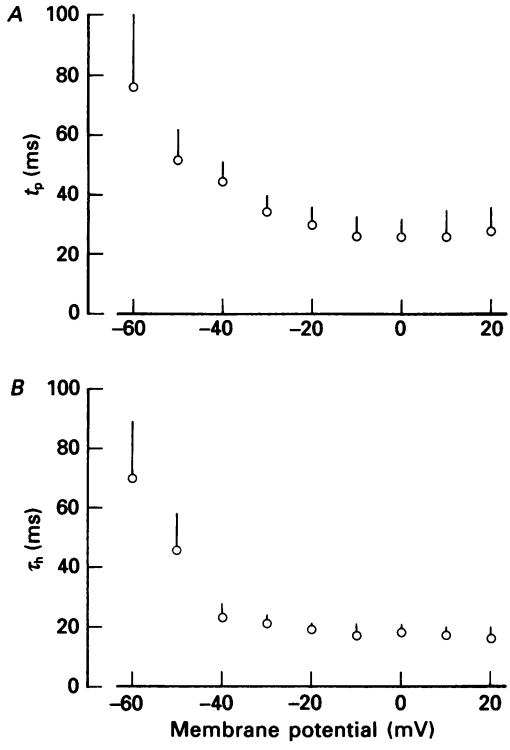

Fig. 6. Voltage dependence of the activation (*A*) and inactivation (*B*) of $I_{Ca,\,LVA}$. Activation time was measured as time to peak current (t_p). Inactivation time was measured as the time constant of the exponential current decay (τ_h). Data are mean value and ±S.E.M. from measurements on four cells. The V_H was −100 mV; $[Ca^{2+}]_o$, 20 mM.

Effects of Ca^{2+} antagonists on $I_{Ca,\,LVA}$

Polyvalent cations known to be Ca^{2+} antagonists were tested with respect to their action on $I_{Ca,\,HVA}$ and $I_{Ca,\,LVA}$. The V_H was −60 mV for $I_{Ca,\,HVA}$ and −100 mV for $I_{Ca,\,LVA}$. Both $I_{Ca,\,HVA}$ and $I_{Ca,\,LVA}$ were activated in an external solution containing 20 mM-Ca^{2+}. Figure 10 shows the dose–inhibition relationship for $I_{Ca,\,HVA}$ (*A*) and $I_{Ca,\,LVA}$ (*B*). The blocking effects of polyvalent cations on $I_{Ca,\,HVA}$ were in the sequence of (IC_{50} in M): La^{3+} $(8\times10^{-8}) > Cd^{2+}$ $(6\times10^{-6}) > Ni^{2+}$ $(1\times10^{-5}) > Zn^{2+}$ (3×10^{-5}). The effects on $I_{Ca,\,LVA}$ were in the sequence of: La^{3+} $(6\times10^{-7}) > Zn^{2+}$ $(3\times10^{-5}) > Cd^{2+}$ $(4\times10^{-4}) > Ni^{2+}$ (6×10^{-4}). The effects of these polyvalent cations were completely reversible.

We also examined sensitivities of both types of Ca^{2+} channels to four representative types of organic Ca^{2+} antagonists: dihydropyridines (nicardipine or nifedipine), papaverine (verapamil), benzothiazepine (diltiazem) and diphenylpiperazine (flunarizine). Following a 3 min treatment of each Ca^{2+} antagonist, step depolarizations

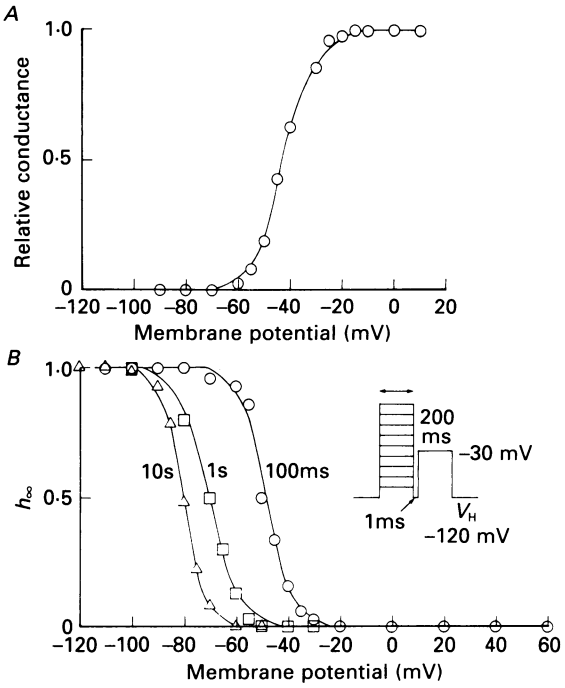

Fig. 7. Voltage dependence of the activation and inactivation for $I_{Ca,\,LVA}$. *A*, activation curve which was deduced by extrapolating the linear part of the corresponding *I–V* curve. A continuous curve was fitted by eye. The V_H was −100 mV. *B*, inactivation of $I_{Ca,\,LVA}$ induced by 100 ms (○), 1 s (□) and 10 s (△) long pre-pulse just before testing depolarization to −30 mV from a V_H of −120 mV. Experimental protocol is shown in the inset. Data shown were obtained from the same cell and are representative of five reproducible experiments. Continuous lines were fitted by the Boltzmann equation:

$$h(V_m) = 1/\{1+\exp(V_m - V_{0.5})k\},$$

using the least-squares method. When the pre-pulse was 100 ms, 1 s and 10 s long, $V_{0.5}$ was −49, −70 and −80 mV, and k was 4·9, 6·0 and 4·0, respectively.

were applied at 30 s intervals. The V_H was −60 mV for $I_{Ca,\,HVA}$ and −100 mV for $I_{Ca,\,LVA}$. The concentration of external Ca^{2+} was 20 mM. Figure 11 shows the dose-dependent inhibition of the organic Ca^{2+} antagonists on $I_{Ca,\,HVA}$ (*A*) and $I_{Ca,\,LVA}$ (*B*). The blocking efficiency for $I_{Ca,\,HVA}$ was as follows (IC_{50} in M): flunarizine (1×10^{-7}) > nicardipine (2×10^{-7}) > verapamil (9×10^{-7}) > diltiazem (3×10^{-6}), while that for $I_{Ca,\,LVA}$ was (IC_{50} in M): flunarizine (2×10^{-7}) > nicardipine (8×10^{-7}) > nifedipine (3×10^{-6}) > diltiazem (3×10^{-5}) > verapamil (7×10^{-5}).

In these experiments we used an external solution containing 20 mM-Ca^{2+}. The effect of Ca^{2+} antagonist on high-voltage-activated Ca^{2+} channels in neurones and

cardiac cells depends on $[Ca^{2+}]_o$ (Akaike, Brown, Nishi & Tsuda, 1981*a*; Lee & Tsien, 1983). Thus, we compared the blocking potency of the Ca^{2+} antagonists at two different $[Ca^{2+}]_o$ values, 2 and 20 mM (Fig. 12). When the external solution had a lower $[Ca^{2+}]_o$, the blocking potency of the organic Ca^{2+} antagonists increased. Such facilitatory effects were observed equally in the two types of Ca^{2+} channels.

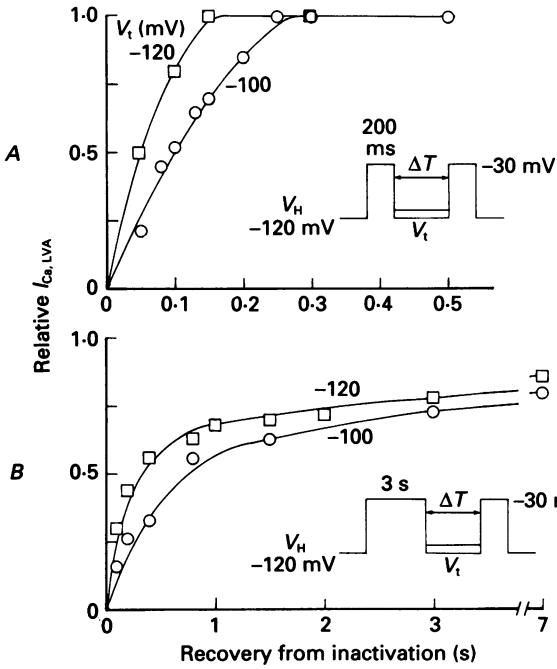

Fig. 8. Recovery from inactivation of $I_{Ca,LVA}$. Time courses of recovery from inactivation induced by 200 ms (*A*) and 3 s (*B*) long pre-pulses to −30 mV at two different repolarization potentials (V_t): −100 (○) and −120 mV (□). Experimental protocols are shown in the insets. The interval time (ΔT) is the duration from the end of the pre-pulse to the test pulse. The amplitude of the current evoked by the pre-pulse was normalized as 1·0. The data were obtained from the same cell and are representative of five reproducible experiments. $[Ca^{2+}]_o$, 20 mM.

One of the dihydropyridine compounds, Bay K 8644 (10^{-6} M), known to be a Ca^{2+} channel agonist, produced about 3-fold augmentation of $I_{Ca,HVA}$ with no effects on $I_{Ca,LVA}$. ω-Conotoxin (10^{-6} M) affected neither $I_{Ca,HVA}$ nor $I_{Ca,LVA}$. Amiloride is a specific blocker of $I_{Ca,LVA}$ in mouse neuroblastoma and chick dorsal root ganglion cells (Tang, Presser & Morad, 1988). Amiloride (10^{-5} M), however, had no effects on $I_{Ca,LVA}$ in cultured vascular SMC.

Population of two types of Ca^{2+} channel in the culture stage

We examined the relationship between the duration of culture and the population of two types of Ca^{2+} channels in cultured vascular SMC. The cultured SMC used in the present experiments proliferated rapidly at the 4th to 5th days of culture and reached confluence on days 13–14. We observed the Ca^{2+} current in less than 10%

of the cells which attained gigaohm seal formation after confluency and in about 80% before the 12th day of culture. Although we could record both types of Ca^{2+} currents just after cell dispersion, the number of cells was too small to study. For these reasons, we used the cells from 6th to 12th days of culture for most of the

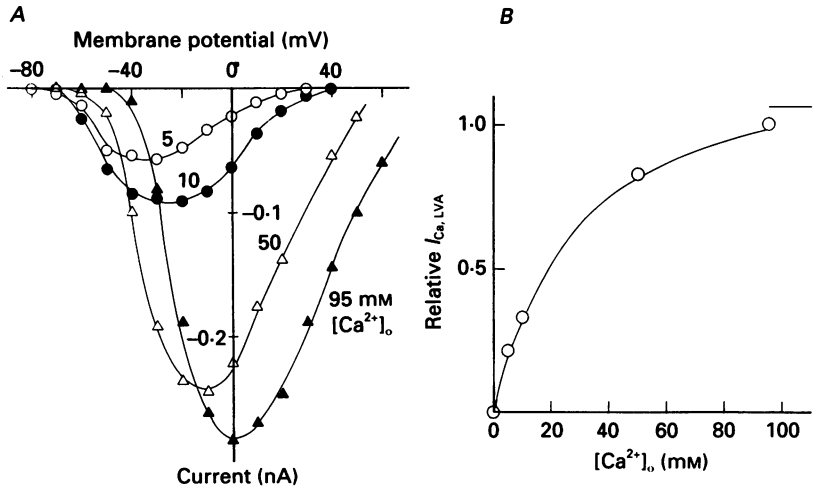

Fig. 9. Dependence of $I_{Ca,\,LVA}$ upon external Ca^{2+} concentration ($[Ca^{2+}]_o$). *A*, *I–V* relationship of $I_{Ca,\,LVA}$ obtained from the same cell in an external solution containing 5, 10, 50 and 95 mM $[Ca^{2+}]_o$. *B*, relationship between the peak amplitude of $I_{Ca,\,LVA}$ and $[Ca^{2+}]_o$. The peak amplitude of $I_{Ca,\,LVA}$ at each concentration was normalized to that of the current at 95 mM $[Ca^{2+}]_o$. A continuous curve was fitted by the Langmuir equation, using the least-squares method. Bar indicates the maximum current level deduced from the Langmuir equation. A definite trend for saturation can be observed but can still not be completed at 95 mM $[Ca^{2+}]_o$. The data were obtained from the same cell and are representative of five reproducible experiments. The V_H was -100 mV.

experiments. Figure 13 shows the relationship between the duration of culture and the ratio of the cells showing $I_{Ca,\,LVA}$ and the total cells showing either type of Ca^{2+} current. In this experiment, F^- was not included in the pipette solution as it might mask $I_{Ca,\,HVA}$. As the cells proliferated, the ratio of cells showing $I_{Ca,\,LVA}$ decreased while that of cells showing $I_{Ca,\,HVA}$ increased.

DISCUSSION

We have demonstrated distinct voltage dependence, kinetics, ionic selectivity and pharmacological properties of the low-voltage-activated Ca^{2+} channels in rat aorta SMC in primary culture. Although the kinetic characteristics of $I_{Ca,\,LVA}$ were identical to those in other preparations (Bean, 1985; Friedman *et al.* 1986; Carbone & Lux, 1987), the $I_{Ca,\,LVA}$ of the cultured SMC was unique in its high sensitivity to some Ca^{2+} antagonists such as flunarizine and nicardipine. In addition, the peak amplitude of $I_{Ca,\,LVA}$ was significantly larger than that of $I_{Ca,\,HVA}$, while the peak amplitude of $I_{Ca,\,LVA}$ in the other preparations was smaller than that of $I_{Ca,\,HVA}$ (Bean, 1985;

Benham *et al.* 1987; Carbone & Lux, 1987; Yatani *et al.* 1987; Hagiwara, Irisawa & Kameyama, 1988).

The, threshold for activation of $I_{Ca,\,LVA}$ in the present experiments was −70 mV in external solution containing 20 mM-Ca^{2+}. This value was more negative than that of $I_{Ca,\,LVA}$ in the aortic A10 cell line (−35 mV recorded with 10 mM-Ca^{2+}; Friedman *et al.* 1986), SMC of the canine saphenous vein (−40 mV with 20 mM-Ca^{2+}; Yatani

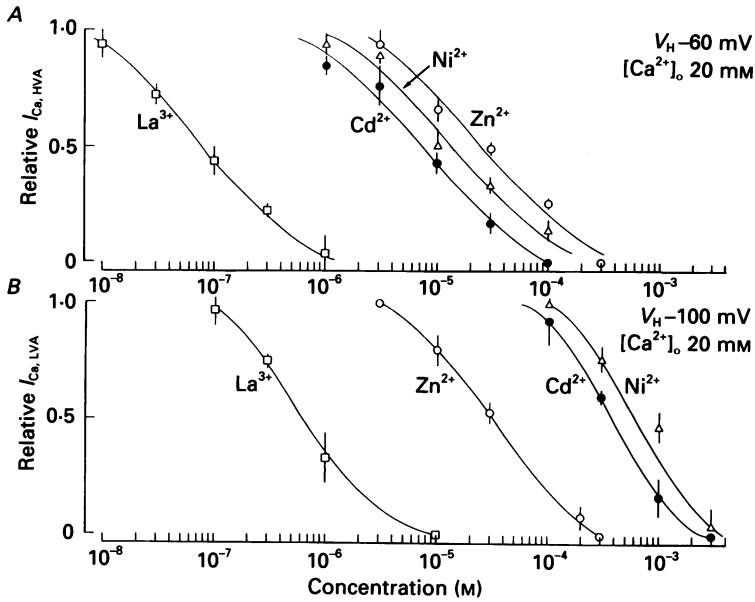

Fig. 10. Dose–response relationships for polyvalent cations in blocking $I_{Ca,\,HVA}$ (*A*) and $I_{Ca,\,LVA}$ (*B*). La^{3+} (□); Cd^{2+} (●); Ni^{2+} (△); Zn^{2+} (○). $I_{Ca,\,HVA}$ was elicited by step depolarizations to +20 mV from a V_H of −60 mV. $I_{Ca,\,LVA}$ was elicited by step depolarizations to −30 mV from a V_H of −100 mV. The duration of the step depolarization was 300 ms. $[Ca^{2+}]_o$ was 20 mM. Step pulses were started 3 min after application of each cation at 30 s intervals. Inhibitory actions of each polyvalent cation were evaluated when the maximum inhibition was attained. The amplitude of the Ca^{2+} current was measured at the peak. The amplitude in the absence of polyvalent cations was normalized as 1·0. In one cell, only one concentration of a cation was examined. Data are mean values obtained from three to six preparations. Vertical lines indicate S.E.M. The V_H was −60 mV for $I_{Ca,\,HVA}$ and −100 mV for $I_{Ca,\,LVA}$.

et al. 1987) or SMC of rat mesenteric arteries (−30 mV with 115 mM-Ba^{2+}; Bean *et al.* 1986). One of the differences in our experimental conditions was that our internal solution contained NMG instead of the Cs^+ commonly used in other reports. Malecot, Feindt & Trautwein (1988) reported that the intracellular NMG shifted the activation curve of $I_{Ca,\,HVA}$ to a negative membrane potential. Thus, NMG might shift the *I–V* relationship of the present $I_{Ca,\,LVA}$ to negative membrane potentials. In fact, we observed a −10 mV shift of the *I–V* relationship of $I_{Ca,\,LVA}$ after 30 min perfusion of MNG. However, in the presence or absence of NMG, the threshold voltage of $I_{Ca,\,LVA}$ was 40 mV more negative than that of $I_{Ca,\,HVA}$. The threshold for activation and the peak membrane potential also depend upon $[Ca^{2+}]_o$. By

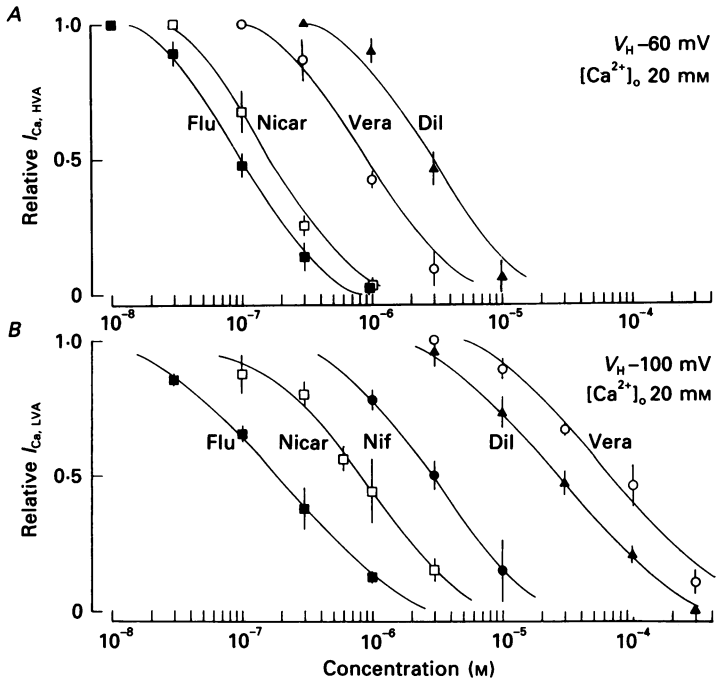

Fig. 11. Dose–response relationships for various organic Ca^{2+} antagonists in blocking $I_{Ca, HVA}$ (*A*) and $I_{Ca, LVA}$ (*B*). Flunarizine (Flu, ■); nicardipine (Nicar, □); verapamil (Vera, ○); diltiazem (Dil, ▲); nifedipine (Nif, ●). $I_{Ca, HVA}$ was elicited by step depolarizations to +20 mV from a V_H of −60 mV. $I_{Ca, LVA}$ was elicited by step depolarizations to −30 mV from a V_H of −100 mV. The duration of the step depolarization was 300 ms. $[Ca^{2+}]_o$ was 20 mM. Step pulses were started 3 min after application of each drug at 30 s intervals. Inhibitory actions of each Ca^{2+} antagonist were measured when the maximum inhibition appeared. The amplitude of the Ca^{2+} current was measured at the peak. The amplitude in the absence of antagonists was normalized as 1·0. Since we could not get a complete recovery despite a drastic wash-out of drugs such as flunarizine, only one dose of the drug was applied to one cell. Data are mean values obtained from three to six preparations. Vertical lines indicate S.E.M. $[Ca^{2}]_o$ was 20 mM.

decreasing $[Ca^{2+}]_o$ from 20 mM to a near-physiological level, the threshold potential shifted to more-negative membrane potentials. Thus, $I_{Ca, LVA}$ of the rat aorta SMC in primary culture may be activated and reach a peak around the resting membrane potential.

We found that some cells had only one type of Ca^{2+} channel; however, other cells had both types of Ca^{2+} channels. Recently, Carbone & Lux (1987) used a high concentration of intracellular F^- to separate $I_{Ca, LVA}$ from $I_{Ca, HVA}$ in the embryonic chick sensory neurone. The intracellular perfusion of F^- for the separation of $I_{Ca, LVA}$ was also successful in the case of hypothalamic neurones isolated acutely from young rats (Akaike, Kostyuk & Osipchuk, 1989). Thus, we perfused the vascular SMC with an internal solution containing 5 mM-F^-, by which only $I_{Ca, HVA}$ was irreversibly blocked within 15 min. The result supports the evidence that high- and low-voltage-activated Ca^{2+} currents in rat aorta SMC in primary culture pass through different Ca^{2+} channels. Intracellular F^- shifts the *I–V* relationship of $I_{Ca, LVA}$ in cultured chick

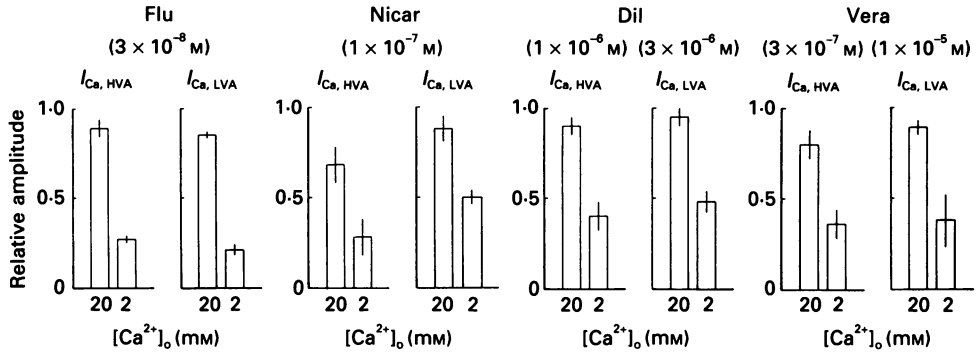

Fig. 12. Relationships between the concentrations of external Ca^{2+} ($[Ca^{2+}]_o$) and the blocking potency of organic Ca^{2+} antagonists on $I_{Ca,\,HVA}$ and $I_{Ca,\,LVA}$. $[Ca^{2+}]_o$ was 20 mM (left columns) or 2 mM (right columns). $I_{Ca,\,HVA}$ was elicited by step depolarizations to +20 mV from a V_H of −60 mV. $I_{Ca,\,LVA}$ was elicited by step depolarizations to −30 mV from a V_H of −100 mV. The amplitude of the Ca^{2+} current was measured at the peak. The amplitude in the absence of organic Ca^{2+} antagonists was normalized as 1·0. We examined the effect of only one Ca^{2+} antagonist in each cell. Data are mean ±S.E.M. obtained from four experiments.

and rat sensory neurones (Carbone & Lux, 1987) and the steady-state inactivation curve of I_A in *Helix* neurones (Tsuda, Oyama, Carpenter & Akaike, 1988) to negative membrane potentials. In the present experiments, using a low concentration of F^-, the *I–V* relationship of $I_{Ca,\,LVA}$ was shifted by only 5 mV, and the kinetics of $I_{Ca,\,LVA}$ were little affected. These results suggest that in vascular SMC also the internal perfusion of 5 mM-F^- is useful to isolate $I_{Ca,\,LVA}$ from $I_{Ca,\,HVA}$.

Low-voltage-activated Ca^{2+} channels in cultured SMC of the rat aorta have approximately equal permeability to Ca^{2+} and Ba^{2+}. This property has been described for $I_{Ca,\,LVA}$ in canine atrial cells (Bean, 1985), the canine saphenous vein (Yatani *et al.* 1987) and rat hypothalamic neurones (Akaike *et al.* 1989). However, in $I_{Ca,\,LVA}$ of the chick and rat sensory neurone (Carbone & Lux, 1987), Ca^{2+} was more permeable than Ba^{2+}. The larger permeability of Sr^{2+} over Ca^{2+} has also been noted in the low-voltage-activated Ca^{2+} channel of rat hypothalamic neurones (Akaike *et al.* 1989).

The inactivation processes of $I_{Ca,\,LVA}$ and $I_{Ca,\,HVA}$ differed in the following ways. Firstly, the inactivation phase of $I_{Ca,\,LVA}$ was fitted by a single-exponential function while that of $I_{Ca,\,HVA}$ was fitted by a sum of two exponential functions. Secondly, the inactivation phases of I_{Ca} and I_{Ba} in the low-voltage-activated channels showed almost the same kinetics, while inactivation of $I_{Ba,\,HVA}$ was slower than that of $I_{Ca,\,HVA}$. Thirdly, the inactivation curve of $I_{Ca,\,LVA}$ did not increase again at positive membrane potentials above the peak membrane potential in the *I–V* curve (−20 mV). The latter two results suggest that the inactivation of $I_{Ca,\,LVA}$ is Ca^{2+}-independent (see Akaike *et al.* 1981*b*; Brown *et al.* 1981; Ganitkevich, Shuba & Smirnov, 1987).

The inactivation process of $I_{Ca,\,LVA}$ was both voltage- and time-dependent. Although $I_{Ca,\,LVA}$ was apparently inactivated completely within 100 ms, about 3 s

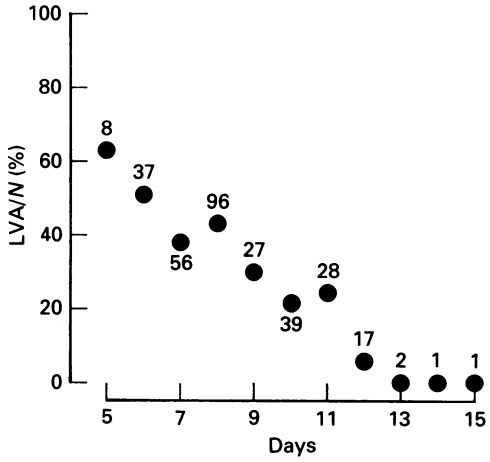

Fig. 13. Relationship between the duration of cell culture and the population of the two types of Ca^{2+} channels. The V_H was -100 mV. The duration of the step depolarization was 300 ms. $[Ca^{2+}]_o$ was 20 mM. 'LVA' indicates the number of the cells showing $I_{Ca,\,LVA}$. N indicates the total number of the cells examined. Horizontal axis indicates the duration of culture. The day zero indicates the day when we seeded cells on the culture dish. The numbers in the figure indicate N at each day.

was needed to attain a complete steady-state inactivation. While the recovery from short inactivation was fitted by a single-exponential function, that from long inactivation was fitted by a sum of two exponential functions. The result suggests that $I_{Ca,\,LVA}$ may time-dependently reach a further inactivation state, from which state a long time would be needed to recover. Biphasic recovery from inactivation has been noted with $I_{Ca,\,HVA}$ of SMC of the guinea-pig taenia caeci (Ganitkevich, Shuba & Smirnov, 1986).

Sensitivity of $I_{Ca,\,LVA}$ and $I_{Ca,\,HVA}$ to inorganic Ca^{2+} antagonists showed the following characteristics: (1) $I_{Ca,\,HVA}$ was more sensitive than $I_{Ca,\,LVA}$ to all the polyvalent cations examined, except Zn^{2+}. (2) La^{3+} suppressed both $I_{Ca,\,HVA}$ and $I_{Ca,\,LVA}$ in the order of 10^{-7} to 10^{-6} M. (3) Ni^{2+} was not a specific blocker of $I_{Ca,\,LVA}$. These results differ from findings in rabbit sino-atrial cells (Hagiwara *et al.* 1988) and frog atrial cell (Bonvallet, 1987), in which Ni^{2+} was a specific blocker of $I_{Ca,\,LVA}$. In the present experiments, both Ni^{2+} and Cd^{2+} at the concentration of 10^{-4} M suppressed only $I_{Ca,\,HVA}$ with no effect on $I_{Ca,\,LVA}$.

Flunarizine and nicardipine acted on $I_{Ca,\,LVA}$ with an IC_{50} of the order of 10^{-8} in 2 mM-Ca^{2+} external solution and differences in blocking potency of flunarizine on $I_{Ca,\,HVA}$ and $I_{Ca,\,LVA}$ were small. Considering the difference in V_H, that is -100 mV for $I_{Ca,\,LVA}$ and -60 mV for $I_{Ca,\,HVA}$, the difference of sensitivity to flunarizine is assumed to be less, because the blocking effect of flunarizine showed a voltage dependence (unpublished observations, T. Kuga & J. Sadoshima). Since it has been reported that $I_{Ca,\,LVA}$ is largely insensitive to organic Ca^{2+} antagonists (Boll & Lux, 1985; Fedulova, Kostyuk & Veselovsky, 1985; Bean *et al.* 1986; Friedman *et al.* 1986; Loirand *et al.* 1986; Benham *et al.* 1987; Yatani *et al.* 1987), $I_{Ca,\,LVA}$ in the rat aorta SMC in primary culture is unique in its high sensitivity to flunarizine and

nicardipine. Recently, dihydropyridine-sensitive $I_{Ca,\,LVA}$ has been also noted in rat isolated hypothalamic neurones (Akaike *et al.* 1989).

$I_{Ca,\,HVA}$ in vascular SMC of the rat aorta is more sensitive to organic Ca^{2+} antagonists than that in visceral SMC, such as rabbit small intestine, in which preparation flunarizine, nicardipine, verapamil and diltiazem suppress $I_{Ca,\,HVA}$ with an IC_{50} of $1{\cdot}4 \times 10^{-6}$, $2{\cdot}4 \times 10^{-8}$, $1{\cdot}3 \times 10^{-6}$ and $1{\cdot}4 \times 10^{-6}$ M, respectively, when recorded in external solution containing 2·5 mM-Ca^{2+} (Terada, Ohya, Kitamura & Kuriyama, 1987*b*; Terada, Kitamura & Kuriyama, 1987*a*). On the contrary, $I_{Ca,\,HVA}$ of this preparation seems to be less sensitive to the dihydropyridine Ca^{2+} antagonist compared with that of vascular SMC in other portions such as rat portal vein (Loirand *et al.* 1986), canine saphenous vein (Yatani *et al.* 1987) and rabbit mesenteric artery (Worley, Deitmer & Nelson, 1986), in which preparations the IC_{50} for the blocking effect of the dihydropyridine Ca^{2+} antagonist was of the order of 10^{-8} M.

In the rat aorta, the IC_{50} of verapamil required to suppress the contraction induced by 65·4 mM-K^+ at 7·5 mM-external Ca^{2+} was $2{\cdot}5 \times 10^{-7}$ M (Karaki, Nakagawa & Urakawa, 1984). Although experimental conditions differed, the IC_{50} of verapamil required to block $I_{Ca,\,HVA}$ at 20 mM-external Ca^{2+} was 9×10^{-7} M in the present experiments. Using Quin-2 microfluorometry, we found that both diltiazem (IC_{50}, $3{\cdot}1 \times 10^{-7}$ M) and verapamil ($4{\cdot}1 \times 10^{-7}$ M) inhibited the elevation of the cytosolic Ca^{2+} induced by high external K^+ at 1 mM-external Ca^{2+}, in the same preparation (Kanaide, Kobayashi, Nishimura, Hasegawa, Shogakiuchi, Matsumoto & Nakamura, 1988). Both drugs had much the same IC_{50} for the suppression of $I_{Ca,\,HVA}$ in the present experiments. These results suggest that $I_{Ca,\,HVA}$ plays an important role as a pathway for Ca^{2+} influx induced by high extracellular K^+.

Since we had no specific organic or inorganic antagonists of $I_{Ca,\,LVA}$, the specific role of $I_{Ca,\,LVA}$ under physiological conditions could not be examined. Because $I_{Ca,\,LVA}$ has a larger amplitude than $I_{Ca,\,HVA}$ and is activated at near resting potential, $I_{Ca,\,LVA}$ might play an important role in near-resting membrane phenomena such as regulation of vascular tone.

In the present experiments, as the cells proliferated, the population with $I_{Ca,\,LVA}$ decreased. It has been reported that it is difficult to record $I_{Ca,\,LVA}$ from aged cultures of embryonic hippocampal neurones (Yaari, Hamon & Lux, 1987) and dorsal root ganglion cells (Carbone & Lux, 1984). Several types of oncogene selectively suppressed low-voltage-activated Ca^{2+} channels in 3T3 fibroblast (Chen, Corbley, Roberts & Hess, 1988). These lines of evidence suggest that $I_{Ca,\,LVA}$ might play some role in proliferation.

We express our thanks to M. Ohara (Kyushu University) for comments on the manuscript; and M. Hasegawa and H. Hisajima for preparing the cell cultures. This investigation was supported by Grants-in-Aid (Nos. 63440037, 63870039, 63113007, 63624005, 63480231, 63624511, 63624510, 63641527, 63113001) from the Ministry of Education, Science and Culture, Japan.

REFERENCES

AKAIKE, N., BROWN, A. M., NISHI, K. & TSUDA, Y. (1981*a*). Actions of verapamil, diltiazem and other divalent cations on the calcium-current of *Helix* neurones. *British Journal of Pharmacology* **74**, 87–95.

AKAIKE, N., KOSTYUK, P. G. & OSIPCHUK, Y. V. (1989). Dihydropyridine-sensitive low-threshold calcium channels in isolated rat hypothalamic neurones. *Journal of Physiology* **412**, 181–195.

AKAIKE, N., LEE, K. S. & BROWN, A. M. (1978). The calcium current of *Helix* neuron. *Journal of General Physiology* **71**, 509–531.

AKAIKE, N., NISHI, K. & OYAMA, Y. (1981*b*). The manganese current of *Helix* neuron. In *The Mechanism of Gated Calcium Transport Across Biological Membranes*, ed. OHNISHI, S. T. & ENDO, M., pp. 111–117. New York: Academic Press.

AKAIKE, N., NISHI, K. & OYAMA, Y. (1983). Characteristics of manganese current and its comparison with currents carried by other divalent cations in snail soma membrane. *Journal of Membrane Biology* **76**, 289–297.

BEAN, B. P. (1985). Two kinds of calcium channels in canine atrial cells. Differences in kinetics, selectivity and pharmacology. *Journal of General Physiology* **86**, 1–30.

BEAN, B. P., STUREK, M., PUGA, A. & HERMSMEYER, K. (1986). Calcium channels in muscle cells isolated from rat mesenteric arteries: modulation by dihydropyridine drugs. *Circulation Research* **59**, 229–235.

BENHAM, C. D., HESS, P. & TSIEN, R. W. (1987). Two types of calcium channels in single smooth muscle cells from rabbit ear artery studied with whole-cell and single channel recordings. *Circulation Research* **61**, suppl. I, I-10–16.

BOLL, W. & LUX, H. D. (1985). Action of organic antagonists on neuronal calcium currents. *Neuroscience Letters* **56**, 335–339.

BONVALLET, R. (1987). A low threshold calcium current recorded at physiological Ca concentrations in single frog atrial cells. *Pflügers Archiv* **408**, 540–542.

BROWN, A. M., MORIMOTO, K., TSUDA, Y. & WILSON, D. L. (1981). Calcium current-dependent and voltage-dependent inactivation of calcium channels in *Helix aspersa*. *Journal of Physiology* **320**, 193–218.

CARBONE, E. & LUX, H. D. (1984). A low voltage-activated calcium conductance in embryonic chick sensory neurons. *Biophysical Journal* **46**, 413–418.

CARBONE, E. & LUX, H. D. (1987). Kinetics and selectivity of a low-voltage-activated calcium current in chick and rat sensory neurones. *Journal of Physiology* **386**, 547–570.

CHEN, C., CORBLEY, M. J., ROBERTS, T. M. & HESS, P. (1988). Voltage-sensitive calcium channels in normal and transformed 3T3 fibroblasts. *Science* **239**, 1024–1026.

FEDULOVA, S. A., KOSTYUK, P. G. & VESELOVSKY, N. S. (1985). Two types of calcium channels in the somatic membrane of new-born rat dorsal root ganglion neurones. *Journal of Physiology* **359**, 431–446.

FISH, R. D., SPERTI, G., COLUCCI, W. S. & CLAPHAM, D. E. (1988). Phorbol ester increases the dihydropyridine-sensitive calcium conductance in a vascular smooth muscle cell line. *Circulation Research* **62**, 1049–1054.

FRIEDMAN, M. E., KURTZ, G. S., KACZOROWSKI, G. J., KATS, G. M. & REUBEN, J. P. (1986). Two calcium currents in a smooth muscle cell line. *American Journal of Physiology* **250**, H699–703.

GANITKEVICH, V. YA., SHUBA, M. F. & SMIRNOV, S. V. (1986). Potential-dependent calcium inward current in a single isolated smooth muscle cell of the guinea-pig taenia caeci. *Journal of Physiology* **380**, 1–16.

GANITKEVICH, V. YA., SHUBA, M. F. & SMIRNOV, S. V. (1987). Calcium-dependent inactivation of potential-dependent calcium inward current in an isolated guinea-pig smooth muscle cell. *Journal of Physiology* **392**, 431–449.

HAGIWARA, N., IRISAWA, H. & KAMEYAMA, M. (1988). Contribution of two types of calcium currents to the pacemaker potentials of rabbit sino-atrial node cells. *Journal of Physiology* **395**, 233–253.

HAMILL, O. P., MARTY, A., NEHER, E., SAKMANN, B. & SIGWORTH, F. J. (1981). Improved patch-clamp techniques for high-resolution current recording from cells and cell-free membrane patches. *Pflügers Archiv* **391**, 85–100.

IRISAWA, H. & KOKUBUN, S. (1983). Modulation by intracellular ATP and cyclic AMP of the slow inward current in isolated single ventricular cells of the guinea-pig. *Journal of Physiology* **338**, 321–337.

KANAIDE, H., KOBAYASHI, S., NISHIMURA, J., HASEGAWA, M., SHOGAKIUCHI, Y., MATSUMOTO, T. & NAKAMURA, M. (1988). Quin2 microfluorometry and effects of verapamil and diltiazem on calcium release from rat aorta smooth muscle cells in primary culture. *Circulation Research* **63**, 16–26.

KARAKI, H., NAKAGAWA, H. & URAKAWA, N. (1984). Comparative effects of verapamil and sodium nitroprusside on contraction and ^{45}Ca uptake in the smooth muscle of rabbit aorta, rat aorta and guinea-pig taenia coli. *British Journal of Pharmacology* **81**, 393–400.

KOBAYASHI, S., KANAIDE, H. & NAKAMURA, M. (1985). Cytosolic-free calcium transients in cultured vascular smooth muscle cells: microfluorometric measurements. *Science* **229**, 553–556.

LEE, K. S. & TSIEN, R. W. (1983). Mechanism of calcium channel blockade by verapamil, D600, diltiazem and nitrendipine in single dialysed heart cells. *Nature* **302**, 790–794.

LOIRAND, G., PACAUD, P., MIRONNEAU, C. & MIRONNEAU, J. (1986). Evidence for two distinct calcium channels in rat vascular smooth muscle cells in short-term primary culture. *Pflügers Archiv* **407**, 566–568.

MALECOT, C. D., FEINDT, P. & TRAUTWEIN, W. (1988). Intracellular *N*-methyl-D-glucamine modifies the kinetics and voltage-dependence of the calcium current in guinea pig ventricular heart cells. *Pflügers Archiv* **411**, 235–242.

STUREK, M. & HERMSMEYER, K. (1986). Calcium and sodium channels in spontaneously contracting vascular muscle cells. *Science* **233**, 475–477.

TANG, C., PRESSER, F. & MORAD, M. (1988). Amiloride selectively blocks the low threshold (*T*) calcium channel. *Science* **240**, 213–215.

TERADA, K., KITAMURA, K. & KURIYAMA, H. (1987*a*). Blocking actions of Ca^{2+} antagonists on the Ca^{2+} channels in the smooth muscle cell membrane of rabbit small intestine. *Pflügers Archiv* **408**, 552–557.

TERADA, K., OHYA, Y., KITAMURA, K. & KURIYAMA, H. (1987*b*). Actions of flunarizine, a Ca^{++} antagonist, on ionic currents in fragmented smooth muscle cells of the rabbit small intestine. *Journal of Pharmacology and Experimental Therapeutics* **240**, 978–983.

TSUDA, Y., OYAMA, Y., CARPENTER, D. O. & AKAIKE, N. (1988). Effects of Ca^{2+} on the transient outward current of single isolated *Helix* central neurones. *British Journal of Pharmacology* **95**, 526–530.

WORLEY III, J. F., DEITMER, J. W. & NELSON, M. T. (1986). Single nisoldipine-sensitive calcium channels in smooth muscle cells isolated from rabbit mesenteric artery. *Proceedings of the National Academy of Sciences of the USA* **83**, 5746–5750.

YAARI, Y., HAMON, B. & LUX, H. D. (1987). Development of two types of calcium channels in cultured mammalian hippocampal neurons. *Science* **235**, 680–682.

YAMAMOTO, H., KANAIDE, H. & NAKAMURA, M. (1983). Metabolism of glycosaminoglycans of cultured rat aortic smooth muscle cells altered during subculture. *British Journal of Experimental Pathology* **64**, 156–165.

YASUI, S. & AKAIKE, N. (1986). Saturation, binding, selectivity and activation energy profile associated with the calcium channel. *Kumamoto Medical Journal* **39**, 105–128.

YATANI, A., SEIDEL, C. L., ALLEN, J. & BROWN, A. M. (1987). Whole-cell and single channel calcium currents of isolated smooth muscle cells from saphenous vein. *Circulation Research* **60**, 523–533.